Middle East Journal of
Scientific Publishing
Vol. (7) Issue (3)
Edition 23th
2024 (1 - 21)

MODEL PHYSICS TO CALCULATE THE THERMAL BUCKLING OF A THIN ECO-CONCRETE PANEL REINFORCED BY COW BONES

Abdelmoutalib BENFRID
Mohamed BACHIR BOUIADJRA
Mohammed CHATBI
Zouaoui Rabie HARRAT
Abdeldjalil BENBAKHTI

Published on: 9 June 2024

Abstract

In the distant past, humans harnessed the skeletal remains of animals to shape their environment. Cow bones, known for their exceptional strength that persists beyond death, slowly decompose over time. Building on this concept, we will explore the thermal buckling characteristics of a concrete slab. By incorporating crushed bovine bone particles after homogenization, in line with the principles of physical energy conservation, we aim to determine the highest temperature at which thermal buckling occurs. This study seeks to understand the thermal behaviour of buckling in concrete plates. Moreover, the widespread local consumption of cows encourages the recycling of bones from commonly eaten animals, aiming to reduce waste from homes and meat markets, lower the risk of harmful bacteria, and investigate potential future uses for these bones. Replacing fine sand with cow bone powder could benefit the economy and mining sectors by reducing environmental damage. Developing a new, efficient, environmentally friendly concrete marks a step forward in exploring alternative materials in concrete research. Mining not only helps conserve natural resources but also

supports the global effort toward environmental preservation and a green economy. Cow bone powder offers concrete significant benefits, promoting a sustainable method to integrate waste recycling into concrete production.

Keywords: Cow Bone Powder, Panel, Thermal Buckling, Eco-friendly concrete.

*** Introduction**

This study delves into the thermal buckling instability of plates made from a novel composite material, specifically concrete reinforced with powdered bovine bones. It seeks to unveil the potential applications and advantages of this material across various domains such as economics, environmental conservation, mining, ecology, energy, and the enhancement of green energy policies. The research is anchored in the expertise of specialists who are deeply engaged with cow bone powder. Their investigations encompassed the production, characterization, and evaluation of the mechanical and tribological performance of composites reinforced with surface-modified cow bone powder. It was discovered that salinization stands out as the optimal method for surface modification, significantly improving the mechanical, thermal, and wear resistance properties. These composites exhibit enhanced performance over their unmodified counterparts in aspects such as glass transition temperature, crystallization, hardness, and tensile strength [1].

The study posits cow bone powder as an economically viable and environmentally friendly material for substituting a portion of cement in concrete.

Tests reveal that cow bone powder comprises nearly all the constituents of cement, albeit in different proportions.

It was observed that concrete's strength enhances with age, recording the highest average compressive strength at 28 days when cement is partially substituted with cow bone powder [2].

In comparing cow bone powder with demolished concrete within foam concrete, the study identified a significant impact on compressive strength, which increased at 18% and 20% replacements but declined at 25%.

This inclusion also introduces more air into the material, making it well-suited for lightweight construction applications.

The study, while focused on concrete Panels, provides a foundation for future inquiries [3].

Cow bone, treated as bio-waste, has been transformed into an environmentally friendly and economically viable resource. This research utilized cow bone heads that were collected, cleaned, sun-dried, and milled into nanoparticle powder.

Various characterization techniques such as scanning electron microscopy (SEM), energy-dispersive X-ray spectroscopy (EDX), and X-ray fluorescence (XRF) were employed. Image processing techniques enhanced the visual quality and resolution of the final product [4].

Further exploring the utilization of waste materials, the study looked into the additive stabilization of highway lateritic soil with cow bone powder and plastic waste as sub-base materials. Soil samples classified under the CL group and A-6 material showed improved results with the introduction of hydrated lime, cow bone, and plastic waste, highlighting the composite's suitability for highway sub-base material [5]

A study comparing cow bone powder and demolished concrete in foam concrete revealed that cow bone powder significantly impacts compressive strength.

The research indicated that the compressive strength of foam concrete increased with 18% and 20% replacement levels but decreased at 25%. Incorporating cow bone powder also introduces more air into the material, making it suitable for lightweight partitioning.

The study's limitations are confined to concrete Panels; however, it could provide a basis for future research [6].

The research extends into the domain of agricultural waste management in Nigeria, demonstrating how pulverized cow bone ash and waste glass powder (PCBAWGP) enhance the compressive and tensile strength of concrete.

This sustainable method not only reduces CO2 emissions but also extends concrete's lifespan, presenting a viable alternative to Portland cement [7].

Addressing the global issue of bone waste, a bone powder miller was developed to convert cow bone waste into usable materials, thus contributing to waste reduction and sustainable agriculture [8].

The dielectric properties of composite materials from cow bone and carbonized waste were examined, highlighting the improved thermal stability and dielectric properties of carbonized particles [10].

The study further investigated cow bone powder's influence on the slurry suspension of retrograded rice starch for bone repair applications, noting optimized samples showed promising physical properties [11].

Investigations into the potential of waste cow bone and glass as partial cement substitutes in solid concrete bricks revealed that a mixture of beef bone powder and glass powder achieved optimal compressive strength, underscoring the material's environmental friendliness [12].

Additionally, the study ventured into the production of phosphate fertilizer from cow bone waste, highlighting its high P2O5 content and endorsing its chemical efficacy [13].

The sorption efficiency of waste cow bone powder (WCBP) for Pb2+ in aqueous solutions was evaluated, showcasing its potential as a remediation method for lead-contaminated media [15].

Another facet of the research explored the pozzolanic properties of cow dung powder (C.D.P.) as a partial cement replacement in concrete production, finding that a 20% replacement met the strength requirements for lightweight concrete [16].

The effects of incorporating animal bone powder (ABP) as a cement substitute were scrutinized, with findings indicating a significant impact on the mechanical properties of concrete at varying dosages, advocating for an optimal dosage of 10% by weight for concrete mix production [18]

An optimum dosage of 10% by weight is recommended for the production of normal concrete mixes.

Construction industry experts in Ethiopia are endeavoring to enhance the quality and ease of use of materials in construction projects.

Nevertheless, the utilization of alternative materials, such as Ambo Sandstone Fine Aggregate (ASFA), has been limited due to the neglect of proper procedures.

According to Ethiopian standard specifications, quarry samples from SENKELE and ALELTU exhibited high silt content, surpassing 6%.

By removing the silt, the content was reduced to 5.3%, below the

maximum allowed limit of 6%. Consequently, ASFA has been deemed suitable for use in concrete mix production and strength assessment. Priced at 140 ETB per cubic meter, Ambo Sandstone Fine Aggregate is more affordable than river sand. However, it is crucial to wash ASFA thoroughly before its use in construction projects to ensure optimal results [19].

Lastly, the study examined the suitability of Ambo Sandstone Fine Aggregate (ASFA) for concrete production, emphasizing the importance of silt removal and proper preparation for enhancing material quality and performance [20].

This comprehensive investigation, using both experimental and analytical methodologies, contributes significantly to the fields of material science and sustainable construction, offering novel insights into the utilization of cow bone powder and other waste materials in enhancing concrete's thermal and mechanical properties. The primary objective of this study is to develop a mathematical model grounded in physics to investigate the instability of a thin Panel reinforced with fine cow bone particles.

Additionally, the work aims to create a model that assists the field of civil engineering in addressing issues related to biomass concrete.

Furthermore, this research explores the thermal behavior of a novel concrete formulation, thereby contributing to advancements in construction materials.

1- Homogenization by Methods (FU and SHY)[21]

As previously stated in the introduction, the homogenization and the FU and SHY models have been addressed. The following formula determines all properties [21]:-

As previously stated in the introduction, the homogenization and the FU and SHY models have been addressed. The following formula determines all properties [21]:-

$E_H = \zeta_{C.B.P} E_{C.B.P} V_{C.B.P} + E_C V_C$ $\rho_H = \zeta_{C.B.P} \rho_{C.B.P} V_{C.B.P} + \rho_C V_C$	(1)
$\alpha_H = \zeta_{C.B.P} \alpha_{C.B.P} V_{C.B.P} + \alpha_C V_C$ $\lambda_H = \zeta_{C.B.P} \lambda_{C.B.P} V_{C.B.P} + \lambda_C V_C$	(2)
$\nu_H = \zeta_{C.B.P} \nu_{C.B.P} V_{C.B.P} + \nu_C V_C$	(3)

Where: $\zeta_{P.B.C}$ (the effectiveness of cow's bones powders).

$0 \prec \zeta_{C.B.P} \prec 1$	(4)

Moreover, we employ the elasticity formula to ascertain the shear modulus. G_H :

$G_H = \frac{E_H}{2(1+\nu_H)}$	(5)

Knowing that the volume (Matrix plus reinforcement equal one):-

$$V_C + V_{C.B.P} = 1 \quad (6)$$

The effectiveness of reinforcement is determined by the ratio between the minimum and maximum diameters of Cow Bone Particles.

$$\zeta_{P.B.C} = \frac{D_{Min}}{D_{Max}} \quad (7)$$

When:-

$$\zeta_{P.B.C} = \frac{D_{Min}}{D_{Max}} = \frac{950\mu m}{1000\mu m} = 0.95 \quad (8)$$

Table 1. The physical, mechanical, and thermal properties of concrete based on cow bones by rule of homogenization FU SHY [21]

M	V_C *(%)*	$V_{C.B.P}$ *(%)*	*E (GPa)*	*n*	*G (Gpa)*	$a\times10^{-5}$	ρ *(Kg/m³)*	*l (W/mK)*
C [28]	-	-	30	0.3	9.62	1	2500	0.92
C.B.P[29]	-	-	22	0.4	7.86	1.3	2000	0.30
C+10%C.B.P	90	10	29.16	0.31	9.42	1.027	2446	0.857
C+20%C.B.P	80	20	28.31	0.32	9.22	1.055	2392	0.795
C+30%C.B.P	70	30	27.47	0.33	9.03	1.082	2338	0.732

We show from the physics literature to address the problem of determining the critical buckling temperature, a key factor in the study of instability. By defining work and mechanical energy being a scalar quantity we aim for a quantitative characterization of the various forms of motion considered in physics.

The principle of conservation and transformation of energy states that within an isolated system, the total energy, regardless of its form, remains constant [26].

Other study focuses on designing and fabricating a gasifier to produce liquid fuel from plum seeds, specifically Spondias mombin.

The gasifier was constructed using materials selected for their thermal, mechanical, and physical properties.

Performance evaluations were conducted, revealing various parameters such as operating time, fuel combustion rate, and combustion zone temperature [27].

Other work investigates the incorporation of pulverized cow bone ash and waste glass powder (PCBAWGP) in concrete production, demonstrating that this method is sustainable, diminishes waste, and lowers CO2 emissions by reducing the Portland cement content required in cement production.

This strategy is especially advantageous in urban settings [28].

The experiments examined the utilization of burnt and crushed cow

bones (BCCB) as a partial substitute for fine aggregate in concrete.

The results indicated that BCCB acts as a retarder, leading to an increase in the water-cement ratio and compressive strength [29].

In other research investigates the production of phosphate fertilizer from cow bone waste in Indonesian slaughterhouses, concentrating on how the concentrations of phosphoric and sulfuric acid impact the quality of the fertilizer [30].

We will integrate and compare the experimental data with the Young's modulus using the developed law, alongside other empirical formulas, for calculating concrete's behavior at the ultimate limit state.

The study conducted by N. M. Ogarekpe et al. explored the use of burnt and crushed cow bones (BCCB) as a partial substitute for fine aggregate in concrete.

The findings revealed that BCCB acts as a retardant, leading to an increase in the water-cement ratio and a decrease in the average compressive strength, which falls below the recommended minimum strength [30].

Our research contrasts the Young's modulus values as specified in various standards, including the British Standards Institution (BSI) [31], American Concrete Institute (ACI) guidelines [32], concrete in the limit state RBA 60 [33], BAEL 91/99 [34], and the Eurocode 2 (EC2) [35] and (BAEL80) [36]. We focus on the secant modulus of elasticity of concrete, which accounts for instantaneous deformation, comparing it across different international regulations as presented in Table 2. From Figures 1 and 2, it is observed that the modulus of elasticity, as determined by the FU SHY rule developed, allows us to conclude that this rule can provide a safety margin of 15%. This margin serves as an additional indicator for initiating studies through mathematical development, which aligns more closely with reality. All the thermo-mechanical parameters exhibit a gradual decrease with a very slight reduction, maintaining the concrete's stress standard above **25 GPa**.

Table 2: Secant modulus of elasticity of concrete (instantaneous deformation) By the different international regulations with the effective modulus of elasticity (rule of FU SHY).

M	EH [21]	sc28 [30]	EBS I[31]	EACI [32]	ERBA60 [33]	EBAEL80 [36]	EBAEL91/99 [34]	EEC2 [35]
C [28]	30	30	27.96	30.67	38.34	37.28	34.17	30.58
C.B.P[29]	22	-	-	-	-	-	-	-
C+10%C.B.P	29.16	30	27.71	30.26	37.83	37.28	33.87	30.34
C+20%C.B.P	28.31	29.2	27.32	28.00	35.00	36.95	32;16	28.96
C+30%C.B.P	27.47	24.8	26.26	27.88	34.86	34.99	32.08	28.89

Figure 1. Secant modulus of elasticity of concrete (instantaneous deformation) By the different international regulations with the effective modulus of elasticity (rule of FU SHY)

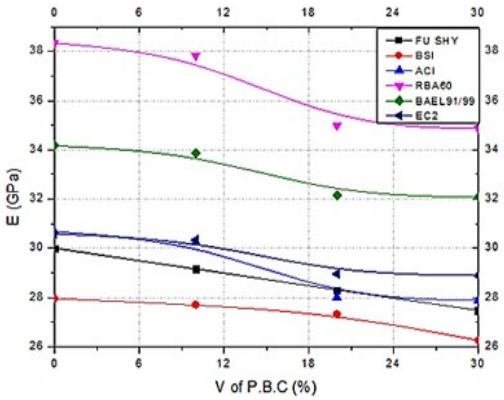

Figure 2. Secant modulus of elasticity of concrete (instantaneous deformation) By the two rules (ACI and EC2), which are very close to the effective elasticity adopted by (The FU SHY rule)

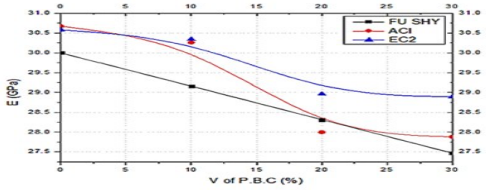

We notice that each time the concentration of cow bone powder particles increases, there is a small decrease in the calculated instantaneous modulus of concrete. The European code standard for the calculation of concrete structures is the closest; thus, the American standard is noted successively as (EC2) and (ACI). So, the FU SHY rule is the closest to homogenizing the mechanical and thermal properties of this new type of concrete.

$E_{ij} = 5.6*(\sigma_{28})^{0.5}$	[32]
$E_{ij} = 22000*(\frac{\sigma_{28}}{10})^{0.3}$	[35]

We would like to highlight some of the work on homogenization that our research team has conducted at the laboratory (LSMAGCTP), such as:-

Benfrid and the team at LSMAGCTP explored the "Thermomechanical Analysis of Glass Powder Based Eco-concrete Panels: Limitations and Performance Evaluation."

This study examines the use of glass powder as an additive in concrete, utilizing Eshelby's model to

determine composite properties and a higher-order shear deformation plate theory for simulation.

The analysis includes the effects of glass powder volume, geometric parameters, and thermal loading, highlighting challenges and suggesting alternative optimization approaches [38] .Benbakhti and al investigated "An Analytical Analysis of the Hydrostatic Bending to Design a Wastewater Treatment Plant Using a New Advanced Composite Material." In response to drought-induced water scarcity, this research focuses on enhancing WWTP structures with nano-tungsten particles in stainless steel. The study uses Mori-Tanaka's homogenization model to analyze hydrostatic bending performance, demonstrating significant improvements in flexural strength with increased tungsten content [39]. Mohammed Chatbi and team examined "Nano-Clay Platelet Integration for Enhanced Bending Performance of Concrete Beams Resting on Elastic Foundation: An Analytical Investigation." This paper explores the reinforcement of concrete beams with various clay nano-platelets using quasi-3D beam theory and Eshelby's model.

The study assesses the static behavior of beams, considering factors like nano-platelet type and volume, providing new insights into structural resistance improvements [40].

HARRET and colleagues studied "Modeling the Thermoelastic Bending of Ferric Oxide (Fe2O3) Nanoparticles-Enhanced RC Slabs." This research presents a refined shear deformation theory for concrete slabs reinforced with Fe2O3 nanoparticles. Using Eshelby's model, the study evaluates the effects of mechanical and thermal loads, showing a 45% reduction in transverse displacement under mechanical loading with Fe2O3 reinforcement [41].

2- The Thermal Buckling (Physic-mathematical model to calculate thermal buckling)

The total energy is written as follows

$$W_{ToT} = W_C + W_P + W_T \quad (8)$$

kinematic kinetic energy

$$W_C^C = \frac{1}{2}\int_V \rho v^2 dv \quad (9)$$

Rotational kinetic energy

$$W_C^R = \sum_{i=1}^{k}\left(\frac{m_i v_i^2}{2} + \frac{m_i (v_i - v_c)^2}{2}\right) \quad (10)$$

So, the overall kinetic energy is written

$$W_C = \frac{1}{2}\left(\frac{mv^2}{2} + \frac{J\omega^2}{2}\right) \quad (11)$$

Internal and external potential energy.

$$W_p = W_p^{out} + W_p^{\text{int}} \quad (12)$$

Internal and external potential energy with rotation

$$W_P = \frac{1}{2}\int_V \omega_p dv \quad (13)$$

For a homogeneous, isotropic and elastic body Linearly

$$\xrightarrow[Isotropic]{Elastic} W_P = \frac{\alpha x^2}{2} \quad (14)$$

Rotational

$$\xrightarrow[Isotropic+gravity]{Elastic} W_P = m\varphi \quad (15)$$

The rotation

$$\varphi = -f\frac{M}{r} + C \quad (16)$$

The Gravity

$$g = -f\frac{M}{r^3}r \quad (17)$$

The gravitational gradient is written.

$$g = -grad\varphi = -(\frac{\partial\varphi}{\partial x}i + \frac{\partial\varphi}{\partial y}j + \frac{\partial\varphi}{\partial z}k) \quad (18)$$

The second derivative of gravitational gradient is written

$$\frac{\partial^2\varphi}{\partial x^2} + \frac{\partial^2\varphi}{\partial y^2} + \frac{\partial^2\varphi}{\partial z^2} = -4\pi f\rho \quad (19)$$

We recall that Laplacian is denoted as.

$$\Delta = \frac{\partial^2}{\partial x^2} + \frac{\partial^2}{\partial y^2} + \frac{\partial^2}{\partial z^2} \quad (20)$$

The angulation is defined as follows.

$$\varphi = -f\int_V \frac{\rho dV}{r} \quad (21)$$

Potential Energy.

$$W_P = -f\frac{mM}{r} + mC \quad (22)$$

Thermal Energy

$$W_T = \frac{1}{2}\int_v \phi dv = \int QdT = \frac{1}{2\Delta T}\int_{T1}^{T2} \bar{C}dT \quad (23)$$

Total energy applied to the body (Variation virtual).

$$\delta W_{ToT} = \delta W_C + \delta W_P + \delta W_T \quad (24)$$

Other writing.

$$\delta W_{ToT} = \frac{1}{2}\int_V \delta\rho v^2 dv + \frac{1}{2}\int_V \delta\omega_p dv + \frac{1}{2}\int_v \delta\phi dv \quad (25)$$

The variation of total energy compared to an effective time.

$$\frac{\partial W_{ToT}}{\partial t} = 0 \quad (26)$$

In energy conservation the derivative of total is equal to zero.

$$\frac{\partial(\frac{1}{2}\int_V \rho v^2 dv + \frac{1}{2}\int_V \omega_p dv + \frac{1}{2}\int_v \phi dv)}{\partial t} = 0 \quad (27)$$

For a surface element of a body, the sliding force is written.

$$\delta A = Fdr = Fds\cos\alpha = F_\tau ds \quad (28)$$

The variation of the three forces generated on the body in a system of three axes (x; y; z).

$$\delta A = F_x dx + F_y dy + F_z dz \quad (29)$$

The power efforts or results are given.

$$Nif(x,y,z) = \frac{\delta A}{dt} \quad (30)$$

The sliding effort.

$$Ni = F_{ri}v \quad (31)$$

The rotations or moments results are given.

$$Mi = F_{ri} v * x \quad (32)$$

Axial rotations in space.

$$\frac{\omega_x}{x} = \frac{\omega_y}{y} = \frac{\omega_z}{z} \quad (33)$$

Speeds in Space in Cartesian Frame.

$$\begin{aligned} v_x &= \dot{x} \\ v_y &= \dot{y} \\ v_z &= \dot{z} \end{aligned} \quad (34)$$

Speeds in General in Cartesian Coordinates.

$$v = \sqrt{\dot{x}^2 + \dot{y}^2 + \dot{z}^2} \quad (35)$$

Speeds in General in Polar Coordinates.

$$v = \sqrt{\dot{r}^2 + (r\dot{\theta})^2 + (r\dot{\phi})\sin\upsilon^2} \quad (36)$$

By combinations we have.

$$\begin{aligned} x &= a * \sin \omega t \\ y &= b * \cos \omega t \\ z &= c * \sin \omega t \end{aligned} \quad (37)$$

Note that.

$$(\frac{x}{a})^2 + (\frac{y}{b})^2 = 1 \quad (38)$$

And.

$$x = a * z \quad (39)$$

In ether to

$$\begin{aligned} x &= r \sin \upsilon * \cos \varphi \quad (40) \\ y &= r \sin \upsilon * \cos \varphi \quad (41) \\ z &= r \cos \upsilon \quad (42) \end{aligned}$$

The Radiation

$$r = \sqrt{x^2 + y^2 + z^2} \quad (43)$$

The Angulation

$$\upsilon = arctg \frac{\sqrt{x^2 + y^2}}{z} \quad (44)$$

By an order of modes, we can write for X axe.

$$\varphi = \frac{m\pi}{a} \quad (45)$$

By an order of modes, we can write for Y axe.

$$\upsilon = \frac{n\pi}{b} \quad (46)$$

The energy accumulation (rigidity) is defined as.

$$K = \int_v V \rho dv \quad (47)$$

By integrating physical work, we can arrive at a field of movement.

$$\begin{aligned} &\int_v xdV; \rightarrow U = u_0 + \frac{\partial w1}{\partial x} + C1\frac{\partial w2}{\partial x} \\ &\int_v ydV; \rightarrow V = v_0 + \frac{\partial w1}{\partial y} + C2\frac{\partial w2}{\partial y} \\ &\int_v zdV; \rightarrow W = w1 + w2 + C3 \\ &C1 = C2 = f(z) \\ &C3 = 0 \end{aligned} \quad (48)$$

The variation in equilibrium state in elasticity [27].

$$\begin{aligned} \delta x &= a_1 x + g_3 y + g_2 x \\ \delta y &= g_3 x + a_2 x + g_1 x \\ \delta z &= g_2 x + g_1 x + a_3 x \end{aligned} \quad (49)$$

The displacements

$$\begin{aligned} a_1 &= \frac{\partial U}{\partial x} \\ a_2 &= \frac{\partial V}{\partial y} \\ a_3 &= \frac{\partial W}{\partial z} \end{aligned} \quad (50)$$

The distortions

$$\begin{aligned} g_1 &= \frac{\partial V}{2\partial z} + \frac{\partial W}{2\partial y} \\ g_2 &= \frac{\partial W}{2\partial x} + \frac{\partial U}{2\partial z} \\ g_3 &= \frac{\partial U}{2\partial y} + \frac{\partial V}{2\partial x} \end{aligned} \quad (51)$$

Compatibility function in step of stability

$$f(x,y,z)=a_1x^2+a_2y^2+a_3z^2 \\ +2g_1yz+2g_2zx+2g_3xy=Cte \quad (52)$$

When

$$1)\delta x=\frac{l}{2}f_x' \quad 2)\delta y=\frac{l}{2}f_y' \quad 3)\delta x=\frac{l}{2}f_z' \quad (53)$$

And

$$\omega_p=h*\frac{x}{L} \quad (54)$$

Energy variation by virtual principle.

$$\partial W_{ToT}=\frac{1}{2}\int_v \partial m g\ddot{x}^2 dv+\frac{1}{2}\int_s \partial h*\frac{x}{L}dv+\frac{1}{2}\int_v \partial Q\Delta T dv \quad (55)$$

Normal stresses are defined in elasticity as follows.

$$\sigma=\frac{dF}{dS} \quad (56)$$

Or.

$$\sigma=K\frac{\Delta x}{x} \quad (57)$$

Lengthening.

$$\nu=\frac{\Delta l}{l} \quad (58)$$

Cutting stresses in rotation.

$$\theta=\tan\theta=\frac{\Delta x}{x} \quad (59)$$

Shear stresses.

$$\tau=G*\theta \quad (60)$$

Shear angle

$$\omega_s=\frac{G\theta^2}{2} \quad (61)$$

The Rigidity.

$$K=\int_v a*b*h*m*gdv \quad (62)$$

In other.

$$\iiint_v \partial\delta W_{ToT} \xrightarrow[u'v+v'u]{\text{int egration}} \begin{bmatrix} K1 & K'1 & K''1 \\ K'1 & K2 & K''2 \\ K''1 & K''2 & K3 \end{bmatrix} \quad (63)$$

Were.

$$K1=D'*(\varphi^4+\upsilon^4+2*\varphi*\upsilon) \\ K2=D'''((\frac{1-\nu}{2})\varphi^2+\upsilon^2)+D'''' \\ K'1=-D''(\varphi^3+\varphi*\upsilon^2) \\ K''1=-D''(\upsilon^3+\upsilon*\varphi^2) \\ K''2=D'''(\frac{1+\nu}{2})\upsilon*\varphi \\ K3=D'''((\frac{1-\nu}{2})\upsilon^2+\varphi^2)+D'''' \quad (64)$$

When

$$D'=\frac{E_H*h^3}{12(1-\nu_H{}^2)} \quad D''=\frac{E_H*A'}{(1-\nu^2)} \\ D'''=\frac{E_H*B'}{(1-\nu_H{}^2)} \quad D''''=\frac{E_H*C'}{(1-\nu_H{}^2)} \quad (65)$$

Their Other.

$$A'=\int_{-h/2}^{h/2} z*f(z)dz \\ B'=\int_{-h/2}^{h/2} f^2(z)dz \\ C'=\int_{-h/2}^{h/2} g^2(z)dz \quad (66)$$

The Flexibility

$$\left[S_{ij}\right]=\begin{bmatrix} K1 & K'1 & K''1 \\ K'1 & K2 & K''2 \\ K''1 & K''2 & K3 \end{bmatrix}-\Delta Tcr\begin{bmatrix} 1 & 0 & 0 \\ 0 & 0 & 0 \\ 0 & 0 & 0 \end{bmatrix} \quad (67)$$

The variation of the critical temperature.

$$\Delta_{Tcr}=solve(DET\left[S_{ij}\right]=0) \quad (68)$$

The high order shear estimation function.

$$f(z)=\frac{1}{8\pi}*\frac{5}{3}*\pi*z*(3-\frac{4*z^2}{h^2}+ \\ 4*\pi*z-4*h*\sin(\frac{\pi*z}{h}) \quad (69)$$

And

$$g(z)=1-f'(z) \quad (70)$$

The variation of the additional critical temperature.

$$\Delta_{TcrAD} = D_0 * \frac{\Delta_{Tc} r * \pi^2 * (1+\nu)}{\alpha_H} * 10^{-3}$$
$$D_0 = \frac{E_H * h^3}{12(1-\nu^2)}$$
$$Smal - Deflexion[37]:$$
$$\Delta_{Tcr} = D_0 * \frac{\Delta_{Tcr} * \pi^2}{E_H * h * \alpha_H} * \left(\frac{m^2}{a^2} + \frac{n^2}{b^2}\right) \quad (71)$$

The surface area and volume of a plate.

$$S = a * b$$
$$V = a * b * h \quad (72)$$

3- The comparison or validation of the Thermal buckling (Physic-mathematical model to calculate thermal buckling)

After carrying out the calculation algorithm with MAPLE 13, we need to compare our findings with those from other research, such as the study on the thermal buckling of a concrete Panelwith simple supports conducted by CHENG X-s [37]. The comparison is detailed in Table 4. It's important to note that S.D. represents the simple deflection method employed by CHENG X-s [37] for conditions where $a_{th}=10^{-5}$ °C and $n=1/6$ and $E=25$ GPa. C.P.T stands for Classical PanelTheory, F.S.D.T represents the First-Order Shear Deformation Theory with a correction coefficient for estimating the shear coefficient. Lastly, H.S.D.T is the Higher-Order Shear Deformation Theory where shear is evaluated through a function dependent on the thickness h and the function for z, as shown in Table 3.

Table 3. The calculation functions for thermal buckling in this work

Function	*S.D*	*C.P.T*	*F.S.D.T*	*H.S.D.T*
f(z)	-	-	z	Eq (67)
g(z)	-	-	$k = \frac{5}{6-\vartheta^2}$	Eq (68)

Table 4. Comparison of calculations by the model created and the results of CHENG X-s [37]

Function	*S.D[37]*	*C.P.T*	*F.S.D.T*	*H.S.D.T*
$b = 1 * a;\ a = 30 * h$	156.6	159.03	158.53	158.96
$b = 3 * a;\ a = 30 * h$	87.1	88.45	88.21	88.33
$b = 1 * a;\ a = 40 * h$	88.1	49.45	89.31	89.43
$b = 3 * a;\ a = 40 * h$	48.9	49.69	49.66	49.69

The results of the selected parameters are in alignment with those reported by CHENG. This study focuses on exploring variations in Panelgeometry and adjustments in reinforcement through the incorporation of cow bone powder at concentrations of 10%, 20%, and 30%.

*** Results and discussions**

We initiated the calculation of the critical temperature leading to instability induced by thermal flame, subsequent to confirming and validating the arithmetic programming, as indicated in Table 4. Initially, our investigation focused solely on ordinary concrete. Then, with each iteration, we augmented the concentration of cow bone particles. The results for ordinary concrete are presented in Table 5, while those for

concentrations of **10%, 20%,** and **30%** of cow bone powder or fine particles are provided in Tables 6, 7, and 8, respectively.We observe that an increase in two geometric ratios leads to a reduction in the critical temperature, resulting in thermal instability. The first ratio is the width-to-length ratio (**b/a**), and the second is the length-to-thickness ratio (**a/h**).

On the other hand, we notice that the discrepancy among the three Paneltheories is minor, possibly attributed to the Panelbeing extremely thin or not very thick. Bone powder exerts a favourable impact on thermal instability by lowering the temperature at which buckling initiates. This signifies a notable advancement in civil engineering, as the thermal resistance enhances with the introduction of this novel concrete derived from bovine waste. When calculating the ratio of the critical temperature of each successive large volume fraction to the preceding one, we discover a consistent coefficient, approximately equal to **0.93**. The most favourable outcomes are achieved with the **30%** cow powder fraction. Since this addition constitutes a BioSource material, we are constrained from exceeding **30%** of such materials.

Table 5. The results of the critical buckling temperature D_{Tcr} of ordinary concrete noted C.

Function	*C.P.T*	*F.S.D.T*	*H.S.D.T*
$a = 30 * h$			
$b = 1.00 * a$	163.38	163.04	163.29
$b = 1.25 * a$	133.97	133.14	133.92
$b = 1.50 * a$	117.97	117.82	117.96
$b = 1.75 * a$	108.36	108.21	108.33
$b = 2.00 * a$	102.11	101.97	10.09
$b = 2.25 * a$	97.82	97.70	97.80
$b = 2.50 * a$	94.76	94.65	94.73
$b = 2.75 * a$	92.49	92.38	92.47
$b = 3.00 * a$	90.76	90.66	90.74
$a = 35 * h$			
$b = 1.00 * a$	120.03	119.84	119.99
$b = 1.25 * a$	98.43	98.30	98.41
$b = 1.50 * a$	86.69	86.59	86.67
$b = 1.75 * a$	79.61	79.53	79.59
$b = 2.00 * a$	74.02	74.95	75.01
$b = 2.25 * a$	71.87	71.79	71.86
$b = 2.50 * a$	69.62	69/55	69.61
$b = 2.75 * a$	67.96	67.89	67.94
$b = 3.00 * a$	66.69	66.63	66.67
$a = 40 * h$			
$b = 1.00 * a$	91.90	91.78	91.87
$b = 1.25 * a$	75.36	75.28	75.34
$b = 1.50 * a$	66.37	66.31	66.93
$b = 1.75 * a$	60.96	60.90	61.36
$b = 2.00 * a$	57.44	57.39	57.44
$b = 2.25 * a$	55.02	54.98	55.01
$b = 2.50 * a$	53.30	53.25	53.30
$b = 2.75 * a$	53.02	52.00	52.01
$b = 3.00 * a$	51.25	51.01	51.04
$a = 45 * h$			
$b = 1.00 * a$	72.61	72.54	72.60
$b = 1.25 * a$	59.54	59.49	59.53
$b = 1.50 * a$	52.44	52.40	52.43
$b = 1.75 * a$	48.16	42.13	48.16
$b = 2.00 * a$	45.38	48.13	45.38
$b = 2.25 * a$	43.48	45.36	43.48
$b = 2.50 * a$	42.11	43.45	42.11
$b = 2.75 * a$	41.10	42.08	41.10
$b = 3.00 * a$	40.34	40.31	40.34

Table 6. The results of the critical buckling temperature D_{Tcr} of ordinary concrete reinforced by 10% with cow bone powder noted C+10%C.B.P.

Function	*C.P.T*	*F.S.D.T*	*H.S.D.T*
$a = 30 * h$			
$b = 1.00 * a$	152.34	152.02	152.26
$b = 1.25 * a$	124.92	124.71	124.86
$b = 1.50 * a$	110.02	109.85	109.98
$b = 1.75 * a$	101.02	100.89	101.01
$b = 2.00 * a$	95.21	95.08	95.17
$b = 2.25 * a$	91.19	91.09	91.18
$b = 2.50 * a$	88.36	88.25	88.31
$b = 2.75 * a$	86.24	86.14	86.21
$b = 3.00 * a$	84.63	84.53	84.61
$a = 35 * h$			
$b = 1.00 * a$	111.92	111.74	111.88
$b = 1.25 * a$	91.78	91.65	91.75
$b = 1.50 * a$	80.84	80.74	80.81
$b = 1.75 * a$	71.23	74.15	74.21
$b = 2.00 * a$	69.95	69.88	69.94
$b = 2.25 * a$	67.01	66.95	67.00
$b = 2.50 * a$	64.81	64.85	64.90
$b = 2.75 * a$	63.37	63.31	63.34
$b = 3.00 * a$	62.18	62.12	61.17
$a = 40 * h$			
$b = 1.00 * a$	85.68	85.58	85.66
$b = 1.25 * a$	70.26	70.19	70.25
$b = 1.50 * a$	61.89	61.82	61.87
$b = 1.75 * a$	56.83	56.77	56.82
$b = 2.00 * a$	53.55	53.51	53.54
$b = 2.25 * a$	51.31	51.27	51.30
$b = 2.50 * a$	49.69	49.68	49.68
$b = 2.75 * a$	48.52	48.47	48.49
$b = 3.00 * a$	47.61	47.58	47.59
$a = 45 * h$			
$b = 1.00 * a$	67.69	67.63	67.68
$b = 1.25 * a$	55.51	55.47	55.50
$b = 1.50 * a$	48.89	48.86	48.89
$b = 1.75 * a$	44.90	44.87	44.88
$b = 2.00 * a$	42.32	42.29	42.31
$b = 2.25 * a$	40.53	40.50	50.53
$b = 2.50 * a$	39.26	39.24	39.26
$b = 2.75 * a$	38.32	38.30	38.33
$b = 3.00 * a$	37.62	37.58	37.61

Table 7. The results of the critical buckling temperature DT_{cr} of ordinary concrete reinforced by 20% with cow bone powder noted C+20%C.B.P.

Function	*C.P.T*	*F.S.D.T*	*H.S.D.T*
$a = 30 * h$			
$b = 1.00 * a$	141.75	141.44	141.68
$b = 1.25 * a$	116.23	116.03	116.18
$b = 1.50 * a$	102.37	102.21	102.33
$b = 1.75 * a$	94.02	93.88	93.98
$b = 2.00 * a$	88.60	88.46	88.56
$b = 2.25 * a$	84.87	84.77	84.84
$b = 2.50 * a$	82.21	82.11	82.19
$b = 2.75 * a$	80.24	80.14	80.22
$b = 3.00 * a$	78.75	78.65	78.72
$a = 35 * h$			
$b = 1.00 * a$	104.15	103.97	104.11
$b = 1.25 * a$	85.40	85.28	85.37
$b = 1.50 * a$	75.21	75.11	75.19
$b = 1.75 * a$	69.07	68.99	69.05
$b = 2.00 * a$	65.08	65.02	65.07
$b = 2.25 * a$	62.35	62.29	62.34
$b = 2.50 * a$	60.39	60.34	60.39
$b = 2.75 * a$	58.96	58.89	58.95
$b = 3.00 * a$	57.86	57.80	57.84
$a = 40 * h$			
$b = 1.00 * a$	79.73	79.64	79.91
$b = 1.25 * a$	65.38	65.31	65.36
$b = 1.50 * a$	57.88	57.53	57.57
$b = 1.75 * a$	49.83	52.84	52.88
$b = 2.00 * a$	47.75	49.79	49.83
$b = 2.25 * a$	46.24	47.79	47.73
$b = 2.50 * a$	45.16	46.21	46.24
$b = 2.75 * a$	44.15	45.10	45.13
$b = 3.00 * a$	44.29	44.26	44.28
$a = 45 * h$			
$b = 1.00 * a$	62.99	62.93	62.98
$b = 1.25 * a$	51.66	51.62	51.65
$b = 1.50 * a$	45.50	45.47	45.48
$b = 1.75 * a$	41.78	41.75	41.78
$b = 2.00 * a$	39.38	39.35	39.37
$b = 2.25 * a$	37.73	37.69	37.71
$b = 2.50 * a$	36.54	36.65	36.53
$b = 2.75 * a$	35.66	35.65	35.66
$b = 3.00 * a$	35.20	34.98	34.99

Table 8. The results of the critical buckling temperature DT_{cr} of ordinary concrete reinforced by 30% with cow bone powder C+30%C.B.P.

Function	*C.P.T*	*F.S.D.T*	*H.S.D.T*
$a = 30 * h$			
$b = 1.00 * a$	132.03	131.75	131.97
$b = 1.25 * a$	108.26	102.08	108.22
$b = 1.50 * a$	95.35	95.21	85.32
$b = 1.75 * a$	87.87	87.45	87.54
$b = 2.00 * a$	82.52	82.41	82.49
$b = 2.25 * a$	79.06	78.95	79.03
$b = 2.50 * a$	76.58	76.48	76.55
$b = 2.75 * a$	74.75	74.65	74.72
$b = 3.00 * a$	73.35	73.26	73.33
$a = 35 * h$			
$b = 1.00 * a$	97.00	96.85	96.97
$b = 1.25 * a$	79.54	79.98	79.52
$b = 1.50 * a$	70.06	69.98	70.03
$b = 1.75 * a$	64.06	64.25	64.32
$b = 2.00 * a$	60.52	60.57	60.61
$b = 2.25 * a$	58.09	58.21	58.07
$b = 2.50 * a$	56.92	56.21	56.25
$b = 2.75 * a$	54.92	54.87	54.91
$b = 3.00 * a$	53.89	53.85	53.88
$a = 40 * h$			
$b = 1.00 * a$	74.27	74.18	74.24
$b = 1.25 * a$	60.89	60.84	60.88
$b = 1.50 * a$	53.64	53.89	53.62
$b = 1.75 * a$	49.26	49.22	49.25
$b = 2.00 * a$	46.41	46.38	46.38
$b = 2.25 * a$	44.46	44.44	44.44
$b = 2.50 * a$	43.07	43.04	43.04
$b = 2.75 * a$	42.04	42.01	42.01
$b = 3.00 * a$	41.27	41.23	41.24
$a = 45 * h$			
$b = 1.00 * a$	58.78	58.62	58.66
$b = 1.25 * a$	48.12	48.08	48.11
$b = 1.50 * a$	42.38	42.35	42.37
$b = 1.75 * a$	38.91	38.89	38.91
$b = 2.00 * a$	36.67	36.65	36.67
$b = 2.25 * a$	35.14	35.12	35.13
$b = 2.50 * a$	34.03	34.02	34.02
$b = 2.75 * a$	33.22	33.20	33.21
$b = 3.00 * a$	32.60	32.52	32.61

* Conclusion

At the conclusion of this study, we can draw the following conclusions:-

1- The optimal volume fraction or concentration of cow bone powder (cow bone particles) yielding favorable results is 30%.

2- This technique enhances the field of civil engineering by introducing eco-concrete, which improves resistance to thermal buckling, thereby promoting energy efficiency in buildings.

3- Cow bone particles have the potential to replace portions of cement in concrete.

4- Reusing cow bones in cement or concrete production offers environmental benefits, given that many countries discard bones from meat processing. Therefore, this concrete can be considered environmentally friendly (eco-friendly).

5- Pozzolanic additives like this powder can reduce $\mathbf{CO_2}$ emissions and heat from cement plants, providing economic advantages alongside environmental benefits.

* Andex

It is important to observe that:

C: Concrete.

C.B.P: Cow bone powder

$\mathbf{V_C}$: Volume of concrete [%].

$\mathbf{V_{C.B.P}}$: Volume Cow bone powder [%].

E: Modulus of elasticity [GPa].

G: Shear's Modulus [GPa].

$\boldsymbol{a}$:Thermal's ratio[$°C^{-1}$].

$\boldsymbol{\rho}$**:** Density [kg m^{-3}].

n:Poisson's ratio.

l: Thermal conductivity [W m^{-1} K^{-1}].

***Z*:** The effectiveness of reinforcement is determined by the ratio between the minimum and maximum diameters of Cow Bone Particles.

D: Diameter of particle.

D_{Max}: maximum diameter of Cow Bone Particles.

D_{Min}: minimum diameter of Cow Bone Particles.

M: Materials.

Eq 01 :

$$E_H = \zeta_{C.B.P} E_{C.B.P} V_{C.B.P} + E_C V_C$$

σ_{28}: the stress of compression at the age of 28 days.

BSI: $E_{ij} = 9100 * (\sigma_{28})^{0.33}$

ACI: $E_{ij} = 5.6 * (\sigma_{28})^{0.5}$

RBA60: $E_{ij} = 7000 * (\sqrt{\sigma_{28}})$

BAEL80: $E_{ij} = 12000 * (\sigma_{28})^{\frac{1}{3}}$

BAEL91/99: $E_{ij} = 11000 * (\sigma_{28})^{\frac{1}{3}}$

EC2: $E_{ij} = 22000 * (\frac{\sigma_{28}}{10})^{0.3}$

a: the length of the plate.

b: the width of the plate.

h: the thickness of the plate.

*** References**

Adewole, T.A., & Oladele, I.O. (2015). Effect of Cow Bone Ash Particle Size Distribution on the Mechanical Properties of Cow Bone Ash-Reinforced Polyester Composites. chemistry and materials research, 7, 40-46. Materials Science, Environmental Science, Engineering chemistry and materials research

Ajibola Ibrahim Quadri and al., (2021) Influence of Cow bone Powder on Cement Partially Substitute in Sandcrete Blocks. Proceedings of the 2021 Annual Conference of the School of Engineering & Engineering Technology, FUTA, 6th – 8th October, 2021

https://www.researchgate.net/publication/355381656

Michelle Daarol, Christian Jan Ariola, Lear Gerbania and Krizer Wrey Yella Napitan B, (2023). First International Conference on Green Energy, Environmental Engineering and Sustainable Technologies 2023 (ICGEST 2023). E3S Web Conf.Volume 455, 2023

https://doi.org/10.1051/e3sconf/202345503026

O. M. Ikumapayi, Esther Titilayo Akinlabi, Paul A. Adedeji & S. A. Akinlabi (2020). Preparation, Characterization, Image

Segmentation and Particle Size Analysis of Cow Bone Powder for Composite Applications.Trends in Manufacturing and Engineering Management pp 273–283.
https://doi.org/10.1007/978-981-15-4745-4_25

Oluwapelumi Olumide Ojuri and al. (2022). Eco-friendly stabilization of highway lateritic soil with cow bone powder admixed lime and plastic granules reinforcement. Cleaner Waste Systems.Volume 2, July 2022, 100012.
https://doi.org/10.1016/j.clwas.2022.100012

Michelle Daarol and al. (2023). Influence of Pulverized Cow Bone as Partial Replacement of Cement and Demolished Concrete as Full Fine Aggregates on Properties of Foam Concrete. E3S Web of Conferences 455.
DOI: 10.1051/e3sconf/202345503026

Adetayo, O.A., Umego, O.M., Faluyi, F. et al.(2022) Evaluation of Pulverized Cow Bone Ash and Waste Glass Powder on the Geotechnical Properties of Tropical Laterite. Silicon 14, 2097–2106 (2022).
https://doi.org/10.1007/s12633-021-00999-4.

Elkin Ronaldo Palomino-Guzmán.(2024). A Sustainable Approach Using Beef and Pig Bone Waste as a Cement Replacement to Produce Concrete. Advances in Sustainable Building and Construction Materials and Structures. Sustainability 2024, 16(2), 701.
https://doi.org/10.3390/su16020701

Bose Mosunmola Edun and al .(2023). Recycling of animal bone as partial replacement for coarse aggregate in lightweight hollow sandcrete blocks. E3S Web of Conferences, 01 (2023),ICMPC 2023/430 219.
https://doi.org/10.1051/e3sconf/202343001219

Omah, A.D., Omah, E.C., Aigbodion, V.S. et al. Characterization of the Thermo-Physical Performance of Bone Particles Proposed for Polymer Composites Production. Natl. Acad. Sci. Lett. 40, 343–347 (2017).
https://doi.org/10.1007/s40009-

017-0592-z Punyanitya, S., Koonawoot, R., Ruksanti, A., Thiensem, S., & Raksujarit, A. (2018). Structure and Mechanical Properties of Retrograded Rice Starch and Cow Bone Powder Composite Sponge. In Materials Science Forum (Vol. 923, pp. 84–88). Trans Tech Publications, Ltd.
https://doi.org/10.4028/www.scientific.net/msf.923.84

A.I. Quadri, A.T. Wasiu, (2020) Assessment of some mechanical properties of concrete by partial replacement of cement with cow bone powder. ournal of Advanced Civil Engineering Practice and Research, 10:10-18
http://ababilpub.com/download/jacepr10-3/

Fasih Ahmed Khan and al. 2015. Utilization of waste glass powder as a partial replacement of cement in concrete. International Journal of Advanced Structures and Geotechnical Engineering. ISSN 2319-5347, Vol. 04, No. 03, July 2015.
https://www.researchgate.net/publication/289537481

A'zam A. Rasulov. (2019). PRODUCTION OF NP FERTILIZERS BASED ON THE DECOMPOSITION OF POOR PHOSPHATES USING A MIXTURE OF PHOSPHORIC AND SULPHURIC ACIDS. lov, Umar K. Alimov, Atanazar R. Seytnazarov, Shafoat S. Namazov, Bokh.
https://journal.uctm.edu/node/j2019-6/17_19-22%20p_1263-1270.pdf

Jonathan Segun Adekanmi. . (2019). PERFORMANCE OF COW DUNG POWDER ON COMPRESSIVE STRENGTH OF BLENDED CONCRETE. Jonathan Segun Adekanmi's Lab Institution: The Federal Polytechnic Ado-Ekiti Department: Civil Engineering.
https://www.researchgate.net/publication/336778591

Jihoon Cha and al. (2010). Kinetic and mechanism studies of the adsorption of lead onto waste cow bone powder (WCBP) surfaces. Environmental Geochemistry and Health.
DOI: 10.1007/s10653-010-9357-z

Sruthy B. (2017). An Experimental Investigation on Strength of Concrete Made with Cow Dung Ash and Glass Fibre. INTERNATIONAL JOURNAL OF ENGINEERING RESEARCH & TECHNOLOGY (IJERT).
DOI: 10.17577/IJERTV6IS030463

Zhaoyang Lu. (2023). Research on the influence of mortar powder content on the performance of recycled concrete. July 2023Journal of Physics Conference Series 2539(1):012033
DOI: 10.1088/1742-6596/2539/1/012033

Abrham Hawaz and al. (2018). Effects of Varying Dosage Replacement of Cement Content by Animal Bone Powder in Normal Concrete Mix Production "Effects of Varying Dosage Replacement of Cement Content by Animal Bone Powder in Normal Concrete Mix Production.". American Journal of Civil Engineering and Architecture, 2018, Vol. 6, No. 4, 133-139 Available online at:
http://pubs.sciepub.com/ajcea/6/4/1
DOI:10.12691/ajcea-6-4-1

Solomon Dagnaw and al. (2021) Study on Partial Replacement of Cement with Animal Bone Ash in Concrete at Elevated Temperatures. Advances of Science and Technology. Solomon Dagnaw's Lab.
DOI: 10.1007/978-3-030-80618-7_1

Woyesa Ararsa. (2018). Suitability of Ambo Sandstone Fine Aggregate as an Alternative River Sand Replacement in Normal Concrete Production. American Journal of Civil Engineering and Architecture.
https://www.researchgate.net/publication/324563914

Fu, S.Y.; Mai, Y.W. (2002); Ching, E.C.Y.; Li, R.K. Correction of the measurement of fiber length of short fiber reinforced thermoplastics. Compos. Part A 2002, 33, 1549–1555.
https://doi.org/10.1016/S1359-835X(02)00114-8

Atteshamuddin S. Sayyad and al. (2004). Thermal buckling of a simply supported moderately thick rectangular FGM plate. Composite Structures 64(2):211-218.

DOI: 10.1016/j.compstruct.2003.08.004

REDDY J.N. (2007). Theory and Analysis of Elastic Plates and Shells, Second Edition, CRC Press (2007 by Taylor & Francis Group, LLC).

TIMOSHENKO & GERE. (1963). Theory of elastic stability 2nd edition; INTERNATIONAL STUDENT EDITION.1963

Handbook of Biomaterial Properties (1998). ISBN: 978-0-412-60330-3

https://link.springer.com/book/10.1007/978-1-4615-5801-9O.

M. Ikumapayi, Esther Titilayo Akinlabi, Paul A. Adedeji & S. A. Akinlabi (2020). Preparation, Characterization, Image Segmentation and Particle Size Analysis of Cow Bone Powder for Composite Applications. Trends in Manufacturing and Engineering Management pp 273–283.

https://doi.org/10.1007/978-981-15-4745-4_25

Oluwapelumi Olumide Ojuri and al. Eco-friendly stabilization of highway lateritic soil with cow bone powder admixed lime and plastic granules reinforcement. Cleaner Waste Systems, Volume 2, July 2022, 100012.

https://doi.org/10.1016/j.clwas.2022.100012

Oluwaseun Adetayo and al. (2022). Performance Evaluation of Ternary Blends of Pulverized Cow Bone Ash and Waste Glass Powder on the Strength Properties of Concrete. VOL. 19 NO. 8 (2022): TRENDS IN SCIENCES, VOLUME 19, NUMBER 8, 15 APRIL 2022.

https://doi.org/10.48048/tis.2022.3222

N. M. Ogarekpe. (2023). Suitability of burnt and crushed cow bones as partial replacement for fine aggregate in concrete. Nigerian Journal of Technology 36(3):686 – 690.

DOI: 10.4314/njt.v36i3.4

N W Sari and al. (2020). A Manufacture of Phosphate Fertilizer from Cow Bones Waste: Phosphate Fertilizer. International Journal of Eco-Innovation in Science and Engineering.

DOI: 10.33005/ijeise.v1i02.27

BS 5628 Code of practice use of masonry: Part I Structural use of

Unreinforced Masonry: BSI, London 1978.
American Concrete Institute (ACI). Committee 440, Guide for the Design and Construction of Externally Bonded Fiber-Reinforced Polymer Systems for Strengthening Unreinforced Masonry Structures, April 2010.
Règles CBA 60 (Reinforced concrete calculation regulations 1960)
Règles BAEL 91 révisées 99 (Reinforced concrete calculation regulations 1991/1999)
Eurocode 2 : Calcul des structures en béton (Reinforced concrete calculation regulations (by European code number 2)
Règles BAEL 80 (Reinforced concrete calculation regulations 1980).
Xuansheng Cheng.(2016) Thermal Elastic Mechanics Problems of Concrete Rectangular Thin Plate.
http://ndl.ethernet.edu.et/bitstream/123456789/75184/1/126.pdf
Benfrid, A., Benbakhti, A., Harrat, Z. R., Chatbi, M., Krour, B., Bouiadjra, M. B. "Thermomechanical Analysis of Glass Powder Based Eco-concrete Panels: Limitations and Performance Evaluation", Periodica Polytechnica Civil Engineering, 67(4), pp. 1284–1297, 2023.
https://doi.org/10.3311/PPci.22781
Benbakhti, A., Benfrid, A., Harrat, Z.R., Chatbi, M., Bouiadjra, M.B., Krour, B. (2024). An analytical analysis of the hydrostatic bending to design a wastewater treatment plant by a new advanced composite material. Revue des Composites et des Matériaux Avancés-Journal of Composite and Advanced Materials, Vol. 34, No. 2, pp. 177-188. https://doi.org/10.18280/rcma.340207
Chatbi, M.; Harrat, Z.R.; Benatta, M.A.; Krour, B.; Hadzima-Nyarko, M.; Işık, E.; Czarnecki, S.; Bouiadjra, M.B. Nano-Clay Platelet Integration for Enhanced Bending Performance of Concrete Beams Resting on Elastic Foundation: An Analytical Investigation. Materials 2023, 16, 5040.
https://doi.org/10.3390/ma16145040
Harrat, Z.R.; Chatbi, M.; Krour, B.; Hadzima-Nyarko, M.; Radu, D.; Amziane, S.; Bachir Bouiadjra, M. Modeling the Thermoelastic

Bending of Ferric Oxide (Fe2O3) Nanoparticles-Enhanced RC Slabs. Materials 2023, 16, 3043. https://doi.org/10.3390/ma16083043